The Electrostatic Contribution to the B to Z Transition of DNA†

Vinod K. Misra and Barry Honig*

Department of Biochemistry and Molecular Biophysics, Columbia University, 630 West 168th Street, New York, New York 10032

Received June 28, 1995; Revised Manuscript Received November 7, 1995⊗

ABSTRACT: In this paper, the finite difference nonlinear Poisson−Boltzmann (NLPB) equation is used to calculate the electrostatic contribution to the B to Z transition of DNA using detailed molecular structures of each DNA form. The electrostatic transition free energy is described as a balance between the change in intramolecular Coulombic interactions and charge-dependent interactions between the DNA and the solvent. As in many prior studies, we find that the larger electrostatic repulsions among the more closely spaced Z-DNA phosphates destabilize this form compared to B-DNA in the absence of solvent. However, as a result of the more compact three-dimensional geometry of Z-DNA, both water and salt are found to strongly stabilize this conformation to the extent that the total electrostatic free energy favors the B to Z transition in aqueous solution. Water acts not only by screening the inter-phosphate repulsions but also by solvating both charged and polar groups on Z-DNA more favorably than B-DNA. In addition, Z-DNA is stabilized by a substantially higher concentration of nearby counterions than B-DNA. The relative stabilization of Z-DNA by salt increases with increasing bulk salt concentration, leading to the high-salt B to Z transition. We find that the salt dependence of the B to Z transition free energy calculated with the NLPB equation agrees reasonably well with experimental results. Since electrostatic interactions are found to favor the Z-form, nonelectrostatic forces must be responsible for the relative stability of B-DNA in solution. An analysis of these forces suggests that the conformational entropy may play an important role.

DNA is a structurally polymorphic macromolecule which, depending on nucleotide sequence and environmental conditions, can adopt a variety of conformations which deviate significantly from canonical B-form DNA. The transition between right-handed B-DNA and left-handed Z-DNA is among the best characterized conformational changes in double-stranded DNA (Jovin et al., 1987; Rich et al., 1984). The difference in stability of B- and Z-DNA has been quantitatively determined as a function of salt concentration (Loprete & Hartman, 1993; Pohl, 1983), base modification (Behe & Felsenfeld, 1981; Zacharias et al., 1988), supercoiling (Stirdivant et al., 1982), water activity (Pohl, 1976; Umehara et al., 1990; Zacharias et al., 1982), temperature (Behe et al., 1985), and pressure (Krzyzaniak et al., 1991). Since atomic resolution single-crystal X-ray diffraction structures exist for both DNA forms [reviewed in Kennard and Hunter (1989)], the B to Z transition is an ideal system for studying the contribution of various forces to the conformational free energy of different DNA structures in solution.

Electrostatic interactions play a crucial role in the transition from B-DNA to Z-DNA. As a result, the equilibrium between the two states depends strongly on salt concentration, with the formation of Z-DNA favored at high monovalent salt concentrations (Pohl, 1983). Many theoretical studies have attempted to account for this observation. It has been shown that the larger electrostatic repulsions among the more closely spaced Z-DNA phosphates destabilize this form relative to B-DNA (Kollman et al., 1982; Matthew & Richards, 1984; Pack & Klein, 1984; Pack et al., 1986; Soumpasis, 1988). Furthermore, many theoretical studies have shown that cations preferentially accumulate around Z-DNA as bulk salt concentration increases (Fenley et al., 1990; Frank-Kamenetskii et al., 1985; Hirata & Levy, 1989; Klement et al., 1991; Matthew & Richards, 1984; Pack & Klein, 1984; Soumpasis, 1984). Thus, a plausible explanation of the salt dependence of the B to Z transition is that the Coulombic repulsions among Z-DNA phosphates are more effectively screened than B-DNA phosphates at high-salt concentrations (Rich et al., 1984; Wang et al., 1981). However, attempts to account for the salt dependence of the B to Z transition quantitatively have encountered significant difficulties.

The simplest description of electrostatic effects on nucleic acid systems is given by counterion condensation (CC) theory (Manning, 1978; Record et al., 1978). In simple CC theory, DNA is modeled as an infinite linear array of point charges characterized by a dimensionless charge density parameter $\xi = e^2/\epsilon kTb$, where ϵ is the dielectric constant of pure bulk solvent, b is the average distance between phosphate charges projected onto the helix axis, and the other symbols have their standard definitions. In the CC model, the geometry of the DNA is captured only through the description of the axial spacing between phosphate charges. Since the linear charge density of B-DNA (Arnott & Hukins, 1972) is larger than that of Z-DNA (Wang et al., 1981), a greater concentration of counterions accumulates around the B conformation than around the Z conformation (Manning, 1969, 1978). As a result, these models predict that B-DNA should become more stable at high salt. Thus, despite the success of simple counterion condensation (CC) theories in describing the salt dependence of many nucleic acid equilibria, they cannot explain the experimentally observed salt dependence of the

† This work was supported by NIH Grant GM41371.
⊗ Abstract published in *Advance ACS Abstracts,* January 1, 1996.

0006-2960/96/0435-1115$12.00/0

B- to Z-DNA transition (Behe & Felsenfeld, 1981; Soumpasis, 1988).

A numerical version of CC theory has been recently developed to calculate counterion binding fractions and ionic free energies for DNA modeled as a double-helical array of phosphates with coordinates based on the crystallographic structures (Fenley et al., 1990). This analysis shows that a larger Na^+ binding fraction for Z-DNA stabilizes this form relative to the B-form at high univalent salt concentrations. However, a direct comparison to experimental results in the high-salt regime has not been provided.

DNA is also often described by the cylindrical Poisson−Boltzmann (PB) equation in which the nucleic acid is modeled as an infinitely long, uniformly charged cylinder characterized by the radius, *a*, and the average axial charge density, *q* (Alexandrowicz & Katchalsky, 1963; Alfrey et al., 1951; Anderson & Record, 1982, 1990; Frank-Kamenetskii et al., 1985; Fuoss et al., 1951; Marcus, 1955; Soumpasis, 1988). Solutions to the NLPB equation based on these cylindrical models show that the smaller radius of Z-DNA results in a more tightly packed ion atmosphere around Z-DNA relative to B-DNA (Frank-Kamenetskii et al., 1985). Although this is a qualitatively accurate depiction of salt effects on the B to Z transition, such calculations have been found to substantially underestimate the salt dependence of the transition (Frank-Kamenetskii et al., 1985; Soumpasis, 1988). As will be discussed below, the failure of simple cylindrical models arises from their neglect of the three-dimensional shape of the DNA, a factor which can have a strong influence on electrostatic potentials, especially in the vicinity of the DNA grooves (Jayaram et al., 1989; Hecht et al., 1995; Honig & Nicholls, 1995).

Recently, modified cylindrical PB models which incorporate certain geometric features of each DNA conformation have been developed (Demaret & Gueron, 1993). In these models, DNA is also modeled as an infinitely long, uniformly charged cylinder characterized by the radius, *b*, and the average axial charge density, *u*. The mobile ions are partitioned into two distinct layers: an inner "sheath" layer which lies within a defined volume inside the cylinder radius, *b*, and an outer ion atmosphere described by the cylindrical nonlinear Poisson−Boltzmann (NLPB) equation. On the basis of the three-dimensional geometry of the atoms in each DNA form, the volume available to the ions within the sheath layer is modeled to be larger for B-DNA than for Z-DNA. As a result, more counterions accumulate within the sheath around B-DNA so that the ion sheath effectively reduces the charge density of the B-DNA cylinder relative to Z-DNA in proportion to bulk salt concentration. The higher effective charge density of the composite Z-DNA cylinder and its more narrow diameter result in a more concentrated outer ion atmosphere than B-DNA. Composite cylindrical models and a related simple planar model have been shown to give remarkably accurate results for the salt dependence of the B to Z transition using NLPB theory (Demaret & Gueron, 1993; Gueron & Demaret, 1992). However, they are based on the existence of two distinct layers of ions with different properties around the DNA, an assumption that is not easily justified on experimental or theoretical grounds. In particular, the physical basis for the existence of a sheath layer is not evident from calculations of the ion atmosphere around DNA (Jayaram et al., 1989).

A fundamental problem in describing DNA as a simple cylindrical rod is that molecular shape is known to have important effects on electrostatic potentials (Honig & Nicholls, 1995). It has been suggested that the geometric approximations inherent in cylindrical models are responsible for their failure to accurately describe electrostatic effects on the B to Z transition (Demaret & Gueron, 1993; Gueron & Demaret, 1992). In fact, cylindrical models have been shown to underestimate the electrostatic potential around DNA, in part, because they cannot account for the large potentials found within the major and minor grooves of the nucleic acid (Jayaram et al., 1989). Advances in computational methods in the past few years have made it feasible to rapidly solve the NLPB equation to calculate electrostatic potentials and ionic distributions around nucleic acids described in atomic detail (Honig & Nicholls, 1995; Jayaram et al., 1989). The results of these calculations are similar to those predicted by Monte Carlo simulations of the ion atmosphere around detailed molecular models of DNA (Jayaram et al., 1990). More recently, the NLPB equation has been shown to be a very accurate method for calculating the absolute magnitude of the total electrostatic binding free energy (Misra & Honig, 1995), as well as the salt dependence of the experimentally observed binding constant for several minor groove binding antibiotics and DNA binding proteins (Misra et al., 1994a,b; Zacharias et al., 1992).

We report here on the application of numerical solutions to the NLPB equation to evaluate the electrostatic free energy change of the B to Z transition. The accuracy of these solutions is evaluated by comparison to experimental measurements of the salt dependence of the transition. In addition, the effect of the nucleic acid's three-dimensional shape on the relative electrostatic stability of B- and Z-DNA will be analyzed, and the results will be used as a basis for a general discussion of the thermodynamic forces responsible for the relative stability of B-DNA in solution.

METHODS

Theory

The Transition Free Energy. The free energy of the B to Z transition is defined as

$$\Delta\Delta G^\circ_{B\rightarrow Z} = \Delta G^\circ_Z - \Delta G^\circ_B \quad (1)$$

where ΔG°_Z and ΔG°_B represent the total free energy of each DNA conformation. The term $\Delta\Delta G^\circ_{B\rightarrow Z}$ can be partitioned into nonelectrostatic, $\Delta\Delta G^n_{B\rightarrow Z}$, and electrostatic, $\Delta\Delta G^{el}_{B\rightarrow Z}$, contributions so that

$$\Delta\Delta G^\circ_{B\rightarrow Z} = \Delta\Delta G^n_{B\rightarrow Z} + \Delta\Delta G^{el}_{B\rightarrow Z} \quad (2a)$$

where

$$\Delta\Delta G^n_{B\rightarrow Z} = \Delta G^n_Z - \Delta G^n_B \quad (2b)$$

and

$$\Delta\Delta G^{el}_{B\rightarrow Z} = \Delta G^{el}_Z - \Delta G^{el}_B \quad (2c)$$

The term $\Delta\Delta G^n_{B\rightarrow Z}$ depends on changes in hydrophobic interactions, van der Waals contacts, conformational entropy, and vibrational energy upon transition. $\Delta\Delta G^n_{B\rightarrow Z}$ is essentially salt independent while $\Delta\Delta G^{el}_{B\rightarrow Z}$ is fundamentally

salt dependent. Therefore, the salt dependence of total free energy of transition is simply

$$\partial(\Delta\Delta G^{\circ}_{B\rightarrow Z})/\partial(\ln [M^{+}]) = \partial(\Delta\Delta G^{el}_{B\rightarrow Z})/\partial(\ln [M^{+}]) \quad (3)$$

The Electrostatic Free Energy. The electrostatic free energy, ΔG^{el}, of a highly charged macromolecular system in a 1:1 salt solution can be determined with the nonlinear Poisson−Boltzmann (NLPB) equation:

$$\nabla\cdot[\epsilon(\mathbf{r})\nabla\cdot\phi(\mathbf{r})] - \epsilon\kappa^2 \sinh [\phi(\mathbf{r})] + 4\pi e\varrho^{f}(\mathbf{r})/kT = 0 \quad (4)$$

where ϕ is the dimensionless electrostatic potential in units of kT/e in which k is Boltzmann's constant, T is the absolute temperature, e is the proton charge, ϵ is the dielectric constant, and ρ^{f} is the fixed charge density. The term $\kappa^2 = 1/\lambda^2 = 8\pi e^2 I/\epsilon kT$, where λ is the Debye length and I is the ionic strength of the bulk solution. The quantities ϕ, ϵ, κ, and ρ are all functions of the position vector $\mathbf{r}$ in the reference frame of the fixed macromolecule. It has been shown that ΔG^{el} for any system modeled with the NLPB equation is given by the volume integral over all space (Sharp & Honig, 1990a)

$$\Delta G^{el} = \int \{\varrho^{f}\phi^{f}/2 + \varrho^{f}\phi^{m} + \varrho^{m}\phi^{m}/2 - (\varrho^{m}\phi + kTc^{b}[2\cosh(\phi) - 2])\}\, d\nu \quad (5)$$

where ρ^{f} and ρ^{m} are the fixed and mobile charge densities, respectively, and the potential, ϕ, has been split up into contributions from the fixed charges, ϕ^{f}, and the mobile charges, ϕ^{m}.

The electrostatic free energy of a macromolecule, described by eq 5, can be partitioned into salt-independent and salt-dependent terms (Misra et al., 1994b). The salt-independent contribution to ΔG_{el} is given by (Gilson & Honig, 1988; Gilson et al., 1985)

$$\Delta G_{ns} = \Delta G_{c} + \Delta G_{p} = \int (\varrho^{f}\phi^{f}/2)\, d\nu \quad (6)$$

where ΔG_c is the Coulombic interaction free energy among the fixed macromolecular charges defined in a reference state corresponding to a homogeneous medium with a dielectric of ϵ_m and ΔG_p is the interaction of the macromolecular charges with the pure polarizable solvent in the absence of salt. The salt-dependent contribution to ΔG_{el} is given by (Misra et al., 1994b)

$$\Delta G_{s} = \int \{\varrho^{f}\phi^{m} + \varrho^{m}\phi^{m}/2 - (\varrho^{m}\phi + kTc^{b}[2\cosh(\phi) - 2])\}\, d\nu \quad (7)$$

ΔG_s is the interaction free energy of the macromolecular charges with mobile ions in the aqueous environment. A complete physical description of ΔG_s has been given elsewhere (Misra et al., 1994b).

The salt-independent contribution to the total electrostatic free energy, ΔG_{ns}, can be partitioned into two sets of terms: the self-energies of individual macromolecular charged groups, i (e.g., i can represent individual nucleotides or individual atoms), and the pairwise energies between two macromolecular charged groups, i and j (Gilson et al., 1985)

$$\Delta G_{ns} = \sum_{i=1}^{n}\left(\Delta G_{ii}^{ns} + \frac{1}{2}\sum_{j\neq i}^{n}\Delta G_{ij}^{ns}\right) \quad (8)$$

where n is the number of charges in the system. The self-energy terms are given by

$$\Delta G_{ii}^{ns} = \Delta G_{ii}^{c} + \Delta G_{ii}^{p} \quad (9)$$

and the pairwise interaction energies are

$$\Delta G_{ij}^{ns} = \Delta G_{ij}^{c} + \Delta G_{ij}^{p} \quad (10)$$

In this formalism, ΔG_{ij}^{c} is the pairwise Coulombic interaction free energy in a homogeneous medium with a dielectric of ϵ_m; ΔG_{ij}^{p} is the interaction free energy of each charged group with the solvent polarization induced by the other group (the so-called solvent "screening" term). The self-energy terms are exactly analogous to the pairwise interaction terms: ΔG_{ii}^{c} is the Coulombic self-energy in a homogeneous dielectric medium (ΔG_{ii}^{c} is defined to be 0 for an isolated point charge) and ΔG_{ii}^{p} is the interaction of a charged group with the polarization it induces in the solvent (the solvation free energy).

The salt-dependent contribution to the total electrostatic free energy, ΔG_s, can be explicitly partitioned into analogous self and pairwise energies, ΔG_{ii}^{s} and ΔG_{ij}^{s}, only for the linearized form of the PB equation. For the linear PB equation, the term ΔG_{ij}^{s} is the interaction free energy of each group with the ion atmosphere induced by the other group (the Debye−Hückel screening term), and ΔG_{ii}^{s} is the interaction of a group with its induced ion atmosphere. However, this separation of terms is not possible for the NLPB equation since the electrostatic potential of mean force between two charges is not a simple linear function of the mean ion distributions. As a result, salt effects in the NLPB equation are described only through the overall interaction free energy of the macromolecular charges with mobile ions in the aqueous environment, ΔG_s (Misra et al., 1994b).

The breakdown of ΔG_{ns} into self and pairwise free energy terms leads to a more physically intuitive description of the electrostatic free energy in which the solvent-screened Coulombic free energy among the molecular charges is defined as

$$\Delta G_{sc} = \sum_{j\neq i}^{n}\Delta G_{ij}^{c} + \sum_{i=1}^{n}\Delta G_{ii}^{c} + \sum_{j\neq i}^{n}\Delta G_{ij}^{p} \quad (11)$$

and the desolvation free energy of the charged groups in the low dielectric molecular interior is defined as

$$\Delta G_{d} = \sum_{i=1}^{n}\Delta G_{ii}^{p} \quad (12)$$

The total electrostatic free energy of a molecule is then written as

$$\Delta G^{el} = \Delta G_{c} + \Delta G_{p} + \Delta G_{s} = \Delta G_{sc} + \Delta G_{d} + \Delta G_{s} \quad (13)$$

The electrostatic contribution to the B to Z transition free energy is then simply

$$\Delta\Delta G^{el}{}_{B\rightarrow Z} = \Delta G^{el}{}_{Z} - \Delta G^{el}{}_{B} = \Delta\Delta G^{c}{}_{B\rightarrow Z} + \Delta\Delta G^{p}{}_{B\rightarrow Z} + \Delta\Delta G^{s}{}_{B\rightarrow Z} = \Delta\Delta G^{sc}{}_{B\rightarrow Z} + \Delta\Delta G^{d}{}_{B\rightarrow Z} + \Delta\Delta G^{s}{}_{B\rightarrow Z} \quad (14)$$

and the salt dependence of $\Delta\Delta G^{\circ}{}_{B\rightarrow Z}$ is

$$\frac{\partial(\Delta\Delta G^{\circ}_{B\rightarrow Z})}{\partial(\ln [M^{+}])} = \frac{\partial(\Delta\Delta G^{el}_{B\rightarrow Z})}{\partial(\ln [M^{+}])} = \frac{\partial(\Delta\Delta G^{s}_{B\rightarrow Z})}{\partial(\ln [M^{+}])} \quad (15)$$

Molecular Models

The details of the model used to describe DNA in the finite-difference NLPB method have been given in several publications (Gilson et al., 1988; Honig et al., 1993; Jayaram et al., 1989; Sharp & Honig, 1990b; Sharp et al., 1990). The DNA molecules are described in terms of the three-dimensional structures of $d[(C\text{-}G)_2]_n$ with the location of all charges defined by the coordinates of the appropriate atoms. The coordinates of idealized B-DNA double helices were generated from the local coordinates of Arnott and Hukins (1972) using the InsightII software package (Biosym Technologies, Inc.). The coordinates of the Z-DNA double helices were also generated with InsightII from the idealized coordinates for the Z_I conformation of Z-DNA (Wang et al., 1981). Before partial charges were assigned to each atom, protons were added to each molecule and the conformations were energy minimized using the molecular simulation program DISCOVER (Hagler et al., 1979) with all heavy atoms fixed according to the crystallographic structure.

The charges were assigned to the center of each atom and were treated as being embedded in a low dielectric medium (ϵ_m) consisting of the volume enclosed by the solvent-accessible surface of the macromolecule (probe radius = 1.4 Å). Calculations were done using a value of ϵ_m equal to either 2 or 4. The atomic charges and radii were derived from either the AMBER (Weiner et al., 1986) or the OPLS (Jorgensen & Tirado-Rives, 1988; Pranata et al., 1991) force fields. Additionally, model calculations were done in which only the phosphorus atoms were assigned a charge of −1 and atomic sizes were assigned according to the van der Waals radii with implicit hydrogens as given by Alden and Kim (1979). In each case, the surrounding solvent was treated as a continuum with $\epsilon_s = 80$ and a 1:1 electrolyte behaving according to the NLPB equation. A 2.0 Å ion exclusion radius was included.

Complete details of the finite-difference NLPB procedure used to calculate electrostatic potentials around atomic resolution structures of nucleic acids have been previously reported (Jayaram et al., 1989). The finite difference calculations were done using the DelPhi software package (Nicholls et al., 1990) using a 65^3 or 129^3 lattice. In order to minimize errors related to the representation of the molecular surface, the potentials were calculated with a three step focusing technique (Gilson et al., 1988). In the initial calculation, the largest dimension of the macromolecule fills about 23% of the grid, and the potentials at the lattice points on the boundary of the grid are approximated analytically using the Debye−Huckel equation such that $\phi(\infty) = 0$ (Klapper et al., 1986). In two successive steps the grid is made four times finer such that the largest dimension of the macromolecule fills 92% of the grid with the boundary conditions interpolated from the previous step. This technique has been shown to improve the accuracy of the solvent-dependent energies of the macromolecule. For calculations of salt-independent free energies, the final resolution of the DNA on the lattice was at least 2.0 grids/Å. For salt dependent free energies, the final resolution was at least 1.2 grids/Å. At these resolutions, the electrostatic free energies vary by less than 1% with respect to grid placement. Once the potentials are determined numerically, for any combination of dielectric constants, they are substituted into eqs 6 and 7, and a numerical integration is carried out to yield the relevant free electrostatic free energies, as previously described (Gilson & Honig, 1988; Misra et al., 1994b).

The net charge density, $\rho(\mathbf{x})$, the counterion concentration, $\rho^{+}(\mathbf{x})$, and the coion concentration, $\rho^{-}(\mathbf{x})$, at any point in solution, $\mathbf{x}$, were calculated from the potential, $\phi(\mathbf{x})$, and the bulk salt concentration, c_o, using the Boltzmann equations:

$$\varrho(\mathbf{x}) = 2c_o \sinh(\phi(\mathbf{x})) \quad (16)$$

$$\varrho^{+}(\mathbf{x}) = c_o \exp(-\phi(\mathbf{x})) \quad (17)$$

$$\varrho^{-}(\mathbf{x}) = c_o \exp(+\phi(\mathbf{x})) \quad (18)$$

The radially averaged salt concentrations were calculated using the radially averaged electrostatic potential, $\langle\phi(r,z,\theta)\rangle_{z,\theta}$, where r, z, and θ are cylindrical coordinates defined relative to the helix axis.

RESULTS

The Electrostatic Contribution to the B to Z Transition, $\Delta\Delta G^{el}_{B\rightarrow Z}$. In Figure 1a, the calculated value of $\Delta\Delta G^{el}_{B\rightarrow Z}$ for $d(C\text{-}G)_n{\cdot}d(C\text{-}G)_n$ oligonucleotides is plotted as a function of univalent salt concentration in an aqueous solution (ϵ_s = 80). The electrostatic free energy is found to stabilize Z-DNA by 1.12 kcal/mol per base pair relative to B-DNA at 0.01 M bulk salt concentration; its magnitude increases to 1.96 kcal/mol per base pair at 5.0 M bulk salt concentration. To determine the physical basis of these findings, we have partitioned the electrostatic transition free energy into its salt-dependent and salt-independent contributions.

The Salt-Dependent Contribution to $\Delta\Delta G^{el}_{B\rightarrow Z}$. The calculated salt-dependent contribution to the electrostatic transition free energy, $\Delta\Delta G_s$, stabilizes Z-DNA relative to B-DNA, and the magnitude of $\Delta\Delta G_s$ increases with bulk salt concentration. For univalent salt concentrations between 2.0 and 5.0 M, the salt dependence of $\Delta\Delta G_s$ can be directly compared to the experimental results of Pohl (1983). In Figure 1b, the calculated value of $\Delta\Delta G_s$ is plotted as a function of ln $[M^{+}]$ between 2.0 and 5.0 M bulk univalent salt concentration. In this salt range, $\Delta\Delta G_s$ decreases linearly with ln $[M^{+}]$. The slope of the line calculated with the NLPB equation $[\partial(\Delta\Delta G_s)/\partial(\ln [M^{+}]) = -0.3RT/\text{bp}]$ is about half of the experimentally observed slope $[\partial(\Delta\Delta G^{\circ}{}_{B\rightarrow Z})/\partial(\ln [M^{+}]) = -0.6RT/\text{bp}$; Pohl, 1983]; this value 2 orders of magnitude more accurate than results based on the cylindrical PB equation (Frank-Kamenetskii et al., 1985). Our calculated values of $\Delta\Delta G_s$ per base pair vary by less than 5% for oligonucleotide lengths, n, between 12 and 36 bp. This finding agrees with the experimental observation that $\Delta\Delta G^{\circ}{}_{B\rightarrow Z}$ is independent of chain length for $n = 6$ to ∼100 (Pohl, 1983). In addition, the salt-dependent free energies

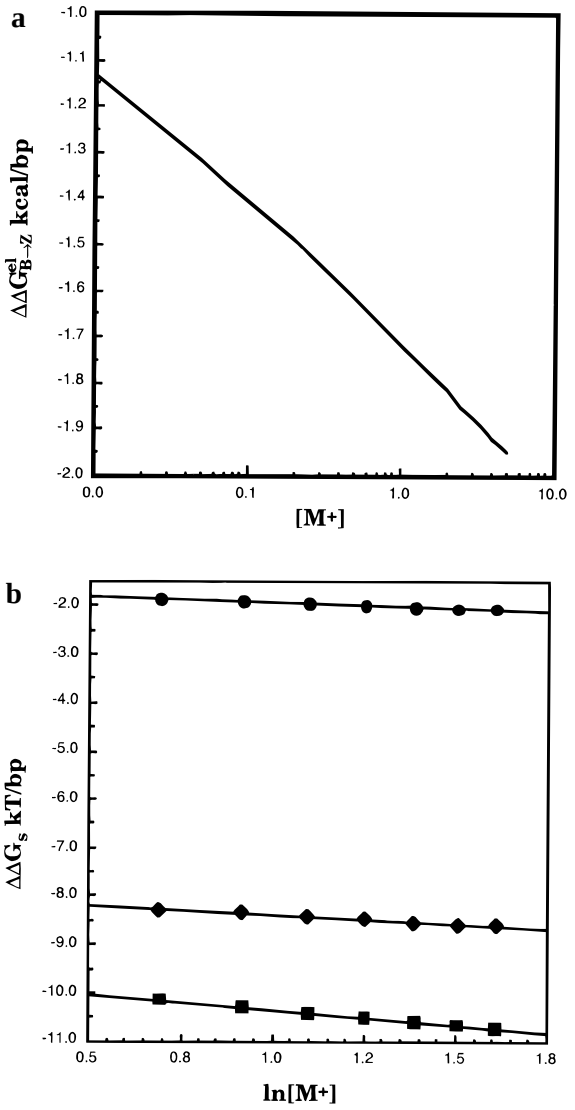

FIGURE 1: (a) Calculated electrostatic contribution to the free energy of the B- to Z-DNA transition as a function of salt concentration. (b) Calculated salt-dependent contribution to the free energy of B-DNA (◆), Z-DNA (■), and the B to Z transition (●) plotted as a function of ln [M^+]. Each line is a linear least-squares regression of the data points.

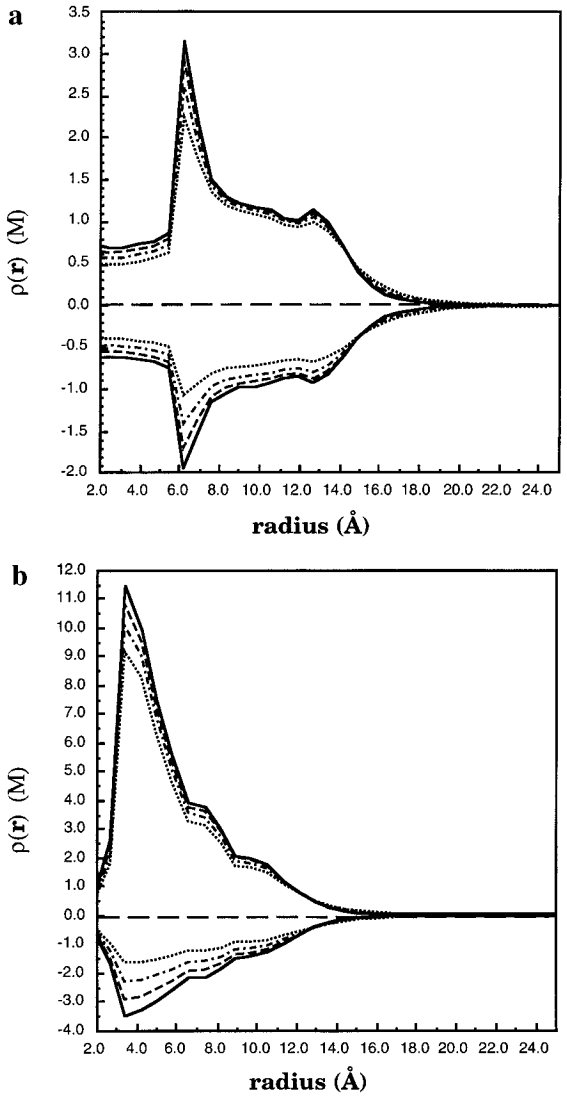

FIGURE 2: Radially averaged excess salt concentration, $\rho(\mathbf{r})$, around (a) B-DNA and (b) Z-DNA plotted at 2.0 M (···), 3.0 M (— · —), 4.0 M (- - -), and 5.0 M (—) bulk salt concentration. The positive concentrations represent the accumulation of cations around the DNA, while the negative concentrations represent the depletion of anions around the DNA at each salt concentration.

vary by less than 2% with the internal dielectric constant ($\epsilon_m = 2$ or 4) and the charge set (AMBER or OPLS).

The distribution of cations and anions around B- and Z-DNA is shown in panels a and b of Figure 2, respectively, for bulk salt univalent concentrations ranging between 2.0 and 5.0 M. Long-range Coulombic forces between DNA and mobile ions in solution drive the formation of the ion atmosphere. The resulting accumulation of cations and depletion of anions (Figure 2) around the DNA electrostatically stabilize the double helix so that ΔG_s is a large negative number for both B- and Z-DNA (Figure 1b). As the bulk salt concentration increases, counterions progressively accumulate while coions progressively diminish near the DNA, so that ΔG_s decreases with increasing [M^+] for each DNA conformation (Figure 1b).

It is clear that the more concentrated, highly structured ion atmosphere around Z-DNA electrostatically stabilizes this structure more strongly than does the atmosphere around B-DNA (Figure 1b). For example, at 2.5 M bulk salt concentration, the ion atmosphere stabilizes the Z-form of $[d(C\text{-}G)_6]_2$ by 13.7 kcal/mol relative to B-DNA (Table 1a). Two effects facilitate the association of counterions with Z-DNA relative to B-DNA. First, the narrow diameter of Z-DNA results in higher electrostatic potentials near its

Table 1: Electrostatic Contributions to the Free Energy of the B to Z Transition of $[d(C\text{-}G)_6]_2$

ϵ_s	$\Delta\Delta G_c$	$\Delta\Delta G_p$	$\Delta\Delta G_{sc}$	$\Delta\Delta G_d$	$\Delta\Delta G_{sb}$	$\Delta\Delta G^{el}_{B\rightarrow Z}$ [b]
(a) Partial Charge Sets[a]						
80	327.2	−335.7	8.9	−17.4	−13.7	−22.2 (−22.8)
40	327.2	−317.1	25.4	−15.3	−26.0	−15.9 (−17.3)
20	327.2	−284.6	54.8	−12.2	−45.0	−2.4 (−2.3)
(b) Formal Charge Set[c]						
80	273.6	−274.7	17.8	−18.9	−10.9	−12.0
40	273.6	−257.7	32.3	−16.4	−20.4	−4.5
20	273.6	−228.9	57.3	−12.6	−34.6	10.1

[a] Calculated with the AMBER parameter set; numbers in parentheses calculated with the OPLS parameter set. All energies in units of kcal/mol. [b] Calculated at 2.5 M M^+. [c] Calculated with each phosphorus atom charged to −1 and all other atoms neutral; atomic sizes assigned using the van der Waals radii with implicit hydrogens as reported by Alden and Kim (1979). All energies in units of kcal/mol.

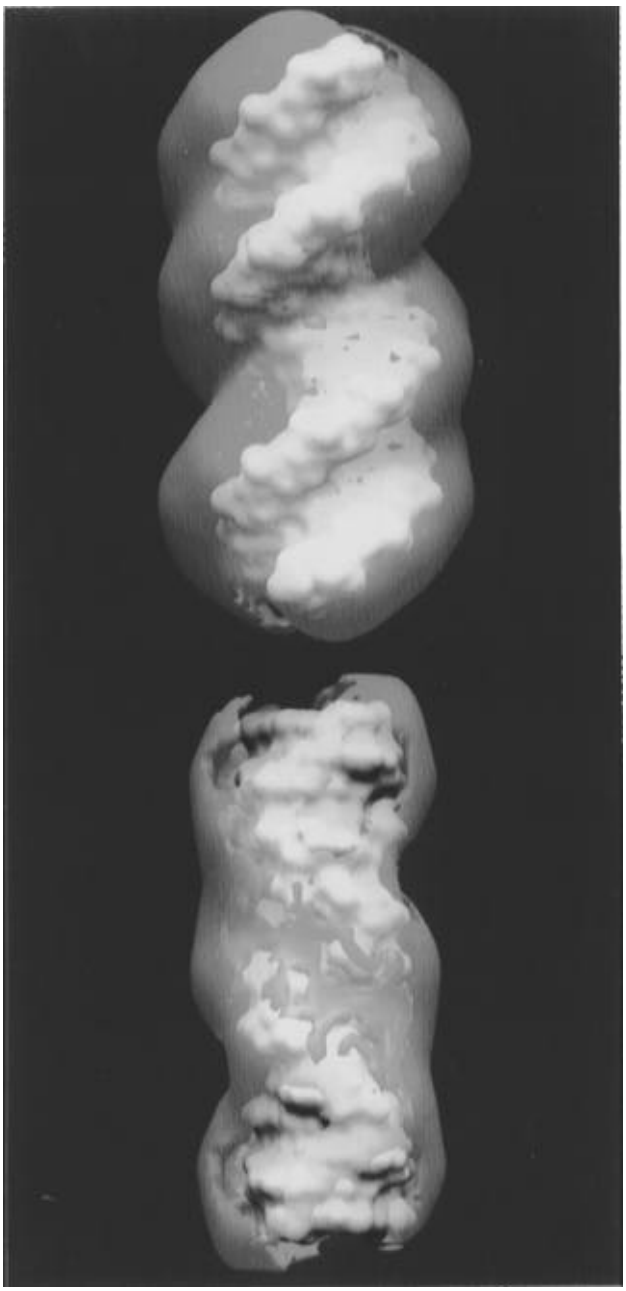

FIGURE 3: Three-dimensional mobile ion charge density contour around (a, top) B-DNA and (b, bottom) Z-DNA at 2.5 M bulk salt concentration. The 1.0 M excess cationic charge density is shown in yellow, and the 6.0 M excess cationic charge density is shown in pink. The solvent-accessible surface is shown in white. The graphical image was created using the GRASP software package (Nicholls et al., 1991).

surface relative to B-DNA, thus enhancing the attraction of the DNA to its counterions. The critical role of the double helix diameter in the description of salt effects around Z-DNA was first noted in cylindrical PB models (Frank-Kamenetskii et al., 1985). Second, the deep minor groove of Z-DNA has a very large negative electrostatic potential which leads to the accumulation of a high concentration of counterions within the groove (Figure 3). The buildup of ions around Z-DNA has been observed in prior PB calculations of the electrostatic potential around B- and Z-DNA (Pack & Klein, 1984; Pack et al., 1986) and is also consistent with calculations based on polymer RISM (Hirata & Levy, 1989) and statistical mechanical theories (Klement et al., 1991). The relative stabilization of Z-DNA by salt slowly decreases with increasing salt concentration since the difference in the number of ions around the two DNA conformations becomes smaller at very high salt concentrations. This effect has also been described previously (Hirata & Levy, 1989).

The Salt-Independent Contributions to $\Delta\Delta G^{el}_{B\rightarrow Z}$. The salt-independent contribution to the electrostatic free energy, $\Delta\Delta G_{ns}$, stabilizes Z-DNA by about 0.7 kcal·mol^{-1}·bp^{-1} relative to B-DNA. In general, the calculated free energy values depend on the atomic charge and size parameters used. We find that the value of $\Delta\Delta G_{ns}$ varies by less than 10% using either the AMBER or OPLS parameter sets (Table 1a) and by less than 5% for oligonucleotide lengths between 12 and 24 base pairs. Furthermore, the qualitative description of electrostatic effects presented here does not depend on the parameters used in the calculations. The results are reported here for a 12 bp oligonucleotide using the AMBER charge set (Weiner et al., 1986) and an internal dielectric constant of 2.

The change in the total Coulombic interaction free energy, $\Delta\Delta G^{c}_{B\rightarrow Z}$, strongly opposes the B to Z transition. As described above, the term $\Delta\Delta G^{c}_{B\rightarrow Z}$ corresponds to hypothetical Coulombic interaction free energy among DNA charges placed in a uniform medium with the same dielectric constant as the DNA itself—i.e., $\Delta\Delta G^{c}_{B\rightarrow Z}$ is calculated in the absence of aqueous solvent. For [d(C-G)$_6$]$_2$, $\Delta\Delta G^{c}_{B\rightarrow Z}$ is calculated to be 327.2 kcal/mol (Table 1a). The electrostatic free energy of transferring the DNA from a homogeneous low dielectric medium into water is given by the solvent polarization free energy, $\Delta\Delta G^{p}_{B\rightarrow Z}$. In other words, the term $\Delta\Delta G^{p}_{B\rightarrow Z}$ corresponds to the electrostatic interaction of the charges in the low dielectric DNA interior with pure water. The change in the solvent polarization free energy, $\Delta\Delta G^{p}_{B\rightarrow Z}$, favors the transition from B-DNA to Z-DNA. For the dodecamer, $\Delta\Delta G^{p}_{B\rightarrow Z}$ is -335.7 kcal/mol in pure water ($\epsilon_s = 80$; Table 1a). As a result of the large favorable solvent contributions, the salt-independent contribution to the electrostatic transition free energy, $\Delta\Delta G_{ns}$, stabilizes the Z-form of [d(C-G)$_6$]$_2$ by 8.5 kcal/mol relative to the B-form (Table 1a; $\Delta\Delta G^{c}_{B\rightarrow Z} + \Delta\Delta G^{p}_{B\rightarrow Z}$) in salt-free water.

In order to better understand the structural origin of these effects, we have partitioned $\Delta\Delta G_{ns}$ into self and pairwise interaction free energies from which the change in the *solvent-screened* Coulombic interaction among the charged nucleotides, $\Delta\Delta G_{sc}$, and the change in the desolvation free energy of each nucleotide upon transition, $\Delta\Delta G_{d}$, were calculated (Table 1a). For [d(C-G)$_6$]$_2$, the change in the Coulombic interaction free energy among the individual nucleotides ($\sum\Delta\Delta G^{c}_{ij}$) opposes the B to Z transition by 369.7 kcal/mol. The large repulsion among the nucleotides results primarily from differences in the distance between the negatively charged phosphate groups on the two DNA forms (Wang et al., 1981). The distance of closest approach between phosphate groups in B-DNA is 11.7 Å, while in Z$_I$-DNA, it is only 7.7 Å. The change in the Coulombic interaction free energy among the atoms within the individual nucleotides ($\sum\Delta\Delta G^{c}_{ii}$) favors the transition by -42.5 kcal/mol. This effect, noted in prior molecular mechanical studies of the B to Z transition (Kollman et al., 1982), results from the greater proximity of the negatively charged phosphate

oxygens to the partially positive atoms of the deoxyribose ring in Z-DNA compared to B-DNA. The sum of the solvent-screening terms ($\sum\Delta\Delta G_{ij}^{p}$) strongly favors the transition by −318.3 kcal/mol so that $\Delta\Delta G_{sc}$ opposes the B to Z transition by only 51.4 kcal/mol in pure water (Table 1a).

Water not only screens the Coulombic interactions among the nucleotides in DNA but also acts by solvating each nucleotide in the B and Z conformation differently. The change in the nucleotide solvation free energy, $\Delta\Delta G_{d}$, favors the Z-form of $[d(C\text{-}G)_6]_2$ by −17.4 kcal/mol relative to the B-form in water (Table 1a). This effect is determined by differences in the burial of both charged and polar groups on each nucleotide in the low dielectric interior of each DNA form. The B to Z transition exposes 1.5 Å^2 of surface area for each nonterminal C·G base pair so that $\Delta\Delta G_{d}$ for each of these base pairs favors the transition by −1.3 kcal/mol.

The Effect of the Solvent Dielectric on $\Delta\Delta G_{B\rightarrow Z}^{el}$. As shown in Table 1a, when the dielectric constant of the surrounding solvent, ϵ_s, is reduced, the electrostatic stability of Z-DNA relative to B-DNA decreases. This effect results from a large decrease in solvent interactions with Z-DNA compared to B-DNA. For $[d(C\text{-}G)_6]_2$, $\Delta\Delta G_{B\rightarrow Z}^{p}$ is reduced from −335.7 kcal/mol in a medium with a dielectric of 80 to −284.6 kcal/mol in a dielectric of 20 (Table 1a). This is due to the large decrease in the screening interactions of the solvent. We find that the solvent-screened Coulombic interaction among the charged nucleotides, $\Delta\Delta G_{sc}$, progressively increases from 51.4 kcal/mol at $\epsilon_s = 80$ to 97.3 kcal/mol at $\epsilon_s = 20$ for $[d(C\text{-}G)_6]_2$ (Table 1a). Reducing the solvent dielectric also decreases the change in the nucleotide solvation free energy, $\Delta\Delta G_{d}$, upon transition (Table 1a). Although there is a concomitant rise in the relative stabilization of Z-DNA by salt, this effect is insufficient to compensate for the large decrease in the screening and solvation of Z-DNA charges (Table 1a). As a result, the electrostatic free energy of transition progressively favors B-DNA as the solvent dielectric is reduced. A similar result has been obtained in prior molecular mechanical studies of the B to Z transition (Kollman et al., 1982).

The Electrostatic Contribution of Individually Charged Phosphates. In order to explicitly determine the role of the charged phosphate backbone in the B to Z transition, we have also calculated the electrostatic contributions to the transition free energy for DNA modeled with a formal charge of −1 on each phophorus atom and all other atoms uncharged. The results of these calculations are shown in Table 1b. As above, inter-phosphate repulsions oppose the B to Z transition of $[d(C\text{-}G)_6]_2$. In aqueous solution ($\epsilon_s = 80$), both water and salt strongly favor Z-DNA relative to B-DNA. Water screens the inter-phosphate repulsions and also solvates individual phosphorus atoms on Z-DNA more favorably than B-DNA. As a result, electrostatic forces are again found to favor the transition from B- to Z-DNA in this model system.

As shown in Table 1b, when ϵ_s is reduced, the stability of Z-DNA relative to B-DNA diminishes due to a large decrease in $\Delta\Delta G_{B\rightarrow Z}^{p}$. This effect is again found to result primarily from a decrease in the screening of coulombic interactions by solvent (with a concomitant increase in $\Delta\Delta G_{sc}$) as well as from the larger decrease in the solvation of the phosphorous atoms of Z-DNA relative to B-DNA. The accompanying increase in $\Delta\Delta G_{B\rightarrow Z}^{s}$ is not sufficient to overcome the decrease in $\Delta\Delta G_{B\rightarrow Z}^{p}$ (Table 1b). While the exact magnitude of the electrostatic transition free energies may depend on the parameter set used, these findings show that the qualitative description of electrostatic effects on the B to Z transition found here are a general property of the three-dimensional geometry of each DNA form rather than the details of any particular parameter set.

DISCUSSION

The equilibrium between different conformers of DNA oligomers is governed by a balance of electrostatic and nonelectrostatic forces. In the following sections we will examine the role of electrostatic interactions in the B to Z transition. In particular, we will discuss the surprising finding that electrostatic forces favor the Z-form of DNA. This result implies that nonelectrostatic forces must be ultimately responsible for the observed stability of B-DNA at physiological salt concentrations. Finally, the nature of these nonelectrostatic forces will be considered.

Salt-Independent Contributions to the B to Z Transition Free Energy. In agreement with many previous studies, Coulombic interactions are found to destabilize Z-DNA relative to B-DNA (Kollman et al., 1982; Matthew & Richards, 1984; Pack & Klein, 1984; Pack et al., 1986; Soumpasis, 1988). In the absence of water, we find that internucleotidyl Coulombic interactions oppose the B to Z transition of $[d(C\text{-}G)_6]_2$ by almost 370 kcal/mol (Table 1a) and that this effect arises primarily from inter-phosphate repulsions (Table 1). Although the Coulombic interactions are reduced by solvent screening, the solvent-screened Coulombic interaction still favors the B-form ($\Delta\Delta G_{sc}$ 8.9 kcal/mol in water; Table 1a). However, water acts not only by screening the inter-phosphate repulsions but also by solvating both charged and polar groups. The change in the solvation free energy upon transition, $\Delta\Delta G_{d}$, is larger than the screened Coulombic term in water ($\epsilon_s = 80$) and is found to preferentially stabilize Z-DNA (Table 1a). Thus, electrostatic forces drive the transition from B- to Z-DNA in an aqueous solution ($\epsilon_s = 80$) even in the absence of salt (Table 1a).

A variety of agents that reduce the activity of water have been found to favor the B to Z transition [reviewed in Rich et al. (1984)]. Our calculations suggest that the effect of reducing water activity is not simply related to a reduction in the dielectric constant of the solvent, ϵ_s, since reducing ϵ_s substantially decreases both solvent screening and solvation of Z-DNA relative to B-DNA (Table 1). Indeed, we find that the overall electrostatic contribution to the relative stability of Z-DNA decreases with smaller values of ϵ_s.

A number of other hypotheses have been made to account for the effects of water activity on the B to Z transition. It has been postulated that lowering the dielectric constant of the solvent results in a nonspecific "clustering" of cations around negatively charged phosphate groups, resulting in a net stabilization of Z-DNA relative to B-DNA (Kollman et al., 1982; Rich et al., 1984). We do, in fact, find that $\Delta\Delta G_{B\rightarrow Z}^{s}$ increases as the dielectric constant decreases. However, this phenomenon, related to the preferential accumulation of cations around Z-DNA, is insufficient to compensate for the large loss in solvent polarization free energy (Table 1). Lowering the dielectric constant may also preferentially enhance site-specific cation binding to Z-DNA

(Dickerson et al., 1982); however, such effects are beyond the scope of our present calculations. Furthermore, it is not apparent that specific ion effects will by themselves be large enough to overcome the large decrease in electrostatic solvent effects observed here.

It has been also proposed that the transition between B- and Z-DNA at low water activities is related to different hydration patterns of the two helical forms (Drew et al., 1980; Westhof, 1988). Specifically, it is been suggested that B-DNA is more highly stabilized than Z-DNA by its surrounding network of water molecules and that the removal of "bound" water molecules preferentially from the phosphate groups of the more favorably hydrated B-DNA helix results in the B to Z transition in low water environments (Saenger et al., 1986; Umehara et al., 1990). However, detailed crystallographic studies indicate that it is difficult to draw any straightforward conclusions about the role of water in the energetics of the B to Z transition from the observed hydration patterns (Gessner et al., 1994; Westhof, 1988).

It appears then that no satisfactory explanation is available to explain the observed effects of water activity on the relative stability of B- and Z-DNA. Of course, water may make both electrostatic and nonelectrostatic contributions to the stability of nucleic acids, and only electrostatic terms have been considered in this work. As discussed below, the essential contribution to the relative stability of B-DNA in solution is also unknown and may well be due to nonelectrostatic effects.

Salt-Dependent Contributions to the B to Z Transition Free Energy. For double-stranded d[$(C\text{-}G)_n$] oligonucleotides, it has been observed that raising the univalent salt concentration above 2.25 M results in a transition from B- to Z-form DNA (Pohl, 1983). It has long been proposed that the preference for the Z-form at high salt concentrations is due to the ionic screening of electrostatic repulsions among the more closely placed phosphate charges in Z-DNA relative to B-DNA (Rich et al., 1984; Wang et al., 1981). Consistent with this notion, the calculations presented here show that the salt-dependent contribution to the electrostatic free energy, $\Delta\Delta G_s$, favors the transition from B- to Z-DNA and that this free energy becomes more favorable with increasing salt concentration. Like the solvent effects discussed above, $\Delta\Delta G_s$ is related to both the increased screening of inter-phosphate repulsions at high-salt concentrations and the more favorable solvation of charged groups on Z-DNA by the ion atmosphere (see eqs 8−10). A comparison of our results to experimental data in similar systems (Pohl, 1983) shows that the finite-difference NLPB model provides a reasonably accurate description of salt-dependent electrostatic effects on the B to Z transition of DNA.

In the NLPB model, salt effects on the B to Z transition are directly related to changes in the distribution of small ions around the DNA. We have shown here that a substantially higher concentration of counterions accumulates around Z-DNA relative to B-DNA because of differences in the three-dimensional geometry of the two DNA forms. Specifically, we find two structural features of Z-DNA which facilitate the association of counterions with this form compared to B-DNA: the relatively narrow diameter of the Z-DNA double helix and the deep minor groove of Z-DNA. The resulting electropositive ion atmosphere stabilizes Z-DNA more strongly than B-DNA. In addition, as bulk salt concentration increases, we find that ions preferentially accumulate around Z-DNA. Therefore, the relative electrostatic stability of Z-DNA progressively increases, ultimately giving rise to the B to Z transition at high salt. Many theoretical studies support this general description of salt effects (Fenley et al., 1990; Frank-Kamenetskii et al., 1985; Hirata & Levy, 1989; Klement et al., 1991; Matthew & Richards, 1984; Pack & Klein, 1984; Soumpasis, 1984).

As discovered in simple cylindrical models, the relatively narrow diameter of Z-DNA is critical in describing salt effects on the B to Z transition (Frank-Kamenetskii et al., 1985). This feature results in a more concentrated, tightly packed ion atmosphere around Z-DNA relative to B-DNA. However, as we have shown here, the extent to which ions differentially accumulate around Z-DNA also depends on the geometry of the grooves in each structure. A simple two-parameter cylindrical model cannot properly describe the accumulation of counterions within the minor groove of Z-DNA. That the more detailed structural model used here more accurately describes salt effects on the B to Z transition than do simple cylindrical NLPB models demonstrates the importance of the molecular shape on electrostatic effects in solution.

As mentioned above, composite cylindrical models and a related simple planar model, which incorporate certain geometric features of DNA, have been shown to give remarkably accurate results for the salt dependence of the B to Z transition using NLPB theory (Demaret & Gueron, 1993; Gueron & Demaret, 1992). However, in contrast to the findings presented here, the interpretation of these models ascribes salt effects on the B to Z transition to the greater accumulation of counterions within the sheath layer around B-DNA rather than to the greater accumulation of ions in the atmosphere around Z-DNA as found here. The physical basis for the existence of a sheath layer is not evident from our calculations.

Shortcomings of the NLPB Model. Several caveats in the interpretation of electrostatic effects on the B to Z transition using the NLPB equation must be kept in mind. The Poisson−Boltzmann (PB) equation provides an approximate but physically complete model of electrostatic interactions in solution. Since the PB equation is based on a mean field theory, it ignores the molecular character of the solvent and treats the system as a dielectric continuum. There are two fundamental approximations with opposing effects inherent in PB theory (Fixman, 1979). The first is the neglect of finite ion size, which results in an overestimation of ion concentrations near the DNA surface. The second approximation is the neglect of electrostatic ion correlations in the potential of mean force, which results in an underestimation of ion concentrations near the DNA surface. It has been shown that these two effects roughly cancel in highly charged systems over a range of univalent salt concentrations extending to at least 0.1 M (Fixman, 1979; Murthy et al., 1985; Vlachy & Haymet, 1986). It has also been shown that adding a repulsive potential to represent ionic size to the mean electrostatic potential accentuates the difference in the accumulation of ions between B- and Z-DNA (Pack & Klein, 1984). By itself, this effect could, in fact, increase the salt dependence of the free energy to improve agreement with the experimental results. However, the relative magnitude of the corrections to the NLPB equation at the high-salt concentrations studied here is uncertain. The role of

these effects in the high-salt B to Z transition remains to be understood at both the experimental and theoretical levels.

It has been suggested that, in addition to the geometric approximations inherent in cylindrical PB models, fundamental simplifications in the PB theory itself are too drastic for an accurate treatment of the B−Z transition (Soumpasis, 1984, 1988). In order to overcome these simplifications, a hypernetted chain theory of ionic solutions in which DNA is modeled as a double helix of phosphate charges has been developed to calculate the salt-dependent stability of Z-DNA (Soumpasis, 1984). In this theory, the salt-dependent variation of the electrostatic free energy of the Z-form relative to B-form DNA in high salt is fitted to the experimental data with an adjustable parameter related to the ionic diameter. However, given the accuracy of our results, it seems that errors associated with cylindrical PB models for DNA are mostly due to the overly simplified representation of the nucleic acid geometry rather than underlying deficiencies in the PB theory itself. Furthermore, the NLPB model uses well-defined theoretical parameters which are not fit to the experimental data.

On the Relative Stability of B-DNA. Perhaps the most surprising result of the calculations presented here is that the electrostatic free energy drives the B to Z transition in aqueous solution. It is clear that the intramolecular Coulombic repulsions between the more closely spaced phosphates across the minor groove of Z-DNA destabilize this form relative to B-DNA in the absence of solvent or salt. However, as a result of the more compact three-dimensional geometry of Z-DNA, both solvent and salt strongly stabilize this conformation. Thus, our calculations predict that elecrostatic interactions favor the Z form at all salt concentrations. The success of the NLPB approach in accounting for the salt dependence of the B to Z transition as well as for other electrostatic properties of DNA (Misra et al., 1994a,b, 1995; Hecht et al., 1995) suggests that this conclusion is likely to be correct. Our results thus strongly suggest that nonelectrostatic forces are primarily responsible for the relative stability of B-DNA compared to Z-DNA. In this picture, the transition occurs when the electrostatic forces favoring the Z-form are equal to the nonelectrostatic forces favoring the B-form. We consider here the specific nonelectrostatic forces which may be responsible for the relative stability of B-DNA.

The contribution of the hydrophobic effect and close packing interactions on the relative stability of each DNA form has not been explicitly determined. However, these forces have been shown to dominate base stacking interactions in nucleic acids (Friedman & Honig, 1995). For the B to Z transition, each of these free energies is approximately proportional to the surface area buried upon transition. We find that the total surface area of a nonterminal d(C)·d(G) base pair in the canonical B-form is only about 1.5 Å^2 smaller than the Z-form. Therefore, the contribution of these forces to the relative stability of B-DNA is expected to be quite small.

The difference in the configurational entropy between the B- and Z-forms has been studied experimentally and theoretically. Measurements of hydrogen-exchange kinetics using NMR (Hartmann et al., 1982; Ramstein & Leng, 1980) and persistence length using dynamic laser light scattering (Thomas & Bloomfield, 1983) suggest that Z-DNA is less conformationally mobile than B-DNA. Vibrational analyses of B- and Z-DNA show that the greater flexibility of the B-DNA entropically stabilizes this form by more than 1 kcal·mol^{-1}·bp^{-1} relative to Z-DNA (Irikura et al., 1985). In addition, the specific arrangement of water molecules around each DNA helix may also contribute to the relative entropic stability of B-DNA (Gessner et al., 1994; Westhof, 1988).

Finally, the intrinsic bond free energies of each DNA form may play a role in the relative stability of B-DNA. In Z-DNA, the deoxyguanosines are in a *syn* conformation with the carbon 3′ in the *endo* conformation, while in B-DNA, each deoxyguanosine is in the *anti* configuration with a C2′ *endo* sugar pucker. There are also more subtle differences in the main-chain torsion angles of the two DNA forms (Dickerson et al., 1982; Wang et al., 1981). However, the accompanying changes in bond-stretching, bond-bending, and torsional free energies have not been determined.

The relative stability of B-DNA in solution depends on a delicate balance of electrostatic and nonelectrostatic free energies. Until now, most theoretical studies have found that both electrostatic and nonelectrostatic free energies stabilize B-DNA relative to Z-DNA. The driving force for the B to Z transition was unclear. We have found here that the electrostatic contribution to the transition free energy favors Z-DNA. At 2.25 M univalent salt concentration, the midpoint of the B to Z transition ($\Delta\Delta G^\circ_{B\rightarrow Z} = 0$) (Pohl, 1983), electrostatic interactions destabilize B-DNA by about 1.0−1.8 kcal·mol^{-1}·bp^{-1} relative to Z-DNA, depending on the parameters used (Table 1). This quantity is of the same order of magnitude as the difference in the vibrational entropy of the two DNA forms (Irikura et al., 1985). Thus, the more unfavorable electrostatic free energy of B-DNA may be offset by its greater entropic stability compared to Z-DNA. However, the precise role of specific water interactions and bond free energies remains to be determined. A complete thermodynamic description of the B to Z transition will depend on a theoretical model which can accurately treat each of these factors in a self-consistent way.

ACKNOWLEDGMENT

We thank Dr. Richard Friedman for his many stimulating and insightful discussions regarding this work.

REFERENCES

Alden, C. J., & Kim, S.-H. (1979) *J. Mol. Biol. 132*, 411−434.
Alexandrowicz, Z., & Katchalsky, A. (1963) *J. Polym. Sci. Part A 1*, 3231−3260.
Alfrey, T. J., Berg, P. W., & Morawetz, H. (1951) *J. Polym. Sci. 7*, 543−547.
Anderson, C. F., & Record, M. T. (1982) *Annu. Rev. Phys. Chem. 33*, 191−222.
Anderson, C. F., & Record, M. T. (1990) *Annu. Rev. Biophys. Biophys. Chem. 19*, 423−465.
Arnott, C. F., & Hukins, D. W. (1972) *Biochem. Biophys. Res. Commun. 47*, 1504−1509.
Behe, M., & Felsenfeld, G. (1981) *Proc. Natl. Acad. Sci. U.S.A. 78*, 1619−1623.
Behe, M. J., Felsenfeld, G., Szu, S. C., & Charney, E. (1985) *Biopolymers 24*, 289−300.
Demaret, J. P., & Gueron, M. (1993) *Biophys. J. 65*, 1700−1713.
Dickerson, R. E., Drew, H. R., Conner, B. N., Wing, R. M., Fratini, A. V., & Kopka, M. L. (1982) *Science 216*, 475−485.
Drew, H., Takano, T., Tanaka, S., Itakura, K., & Dickerson, R. E. (1980) *Nature 286*, 567−573.
Fenley, M. O., Manning, G. S., & Olson, W. K. (1990) *Biopolymers 30*, 1205−1213.
Fixman, M. (1979) *J. Chem. Phys. 70*, 4995−5005.

Frank-Kamenetskii, M. D., Lukashin, A. V., & Anshelevich, V. V. (1985) *J. Biomol. Struct. Dyn. 3*, 35−42.
Fuoss, R. M., Katchalsky, A., & Lifson, S. (1951) *Proc. Natl. Acad. Sci. U.S.A. 37*, 579−589.
Gessner, R. V., Quigley, G. J., & Egli, M. (1994) *J. Mol. Biol. 236*, 1154−1168.
Gilson, M. K., & Honig, B. (1988) *Proteins: Struct., Funct., Genet. 4*, 7−18.
Gilson, M. K., Rashin, A., Fine, R., & Honig, B. (1985) *J. Mol. Biol. 183*, 503−516.
Gilson, M. K., Sharp, K. A., & Honig, B. H. (1988) *J. Comput. Chem. 9*, 327−335.
Gueron, M., & Demaret, J.-P. (1992) *Proc. Nat. Acad. Sci. U.S.A. 89*, 5740−5743.
Hagler, A. T., Stern, P. S., Sharon, R., Becker, J. M., & Naider, F. (1979) *J. Am. Chem. Soc. 101*, 6842−6852.
Hartmann, B., Pilet, J., Ptak, M., Ramstein, J., Malfoy, B., & Leng, M. (1982) *Nucleic Acids Res. 10*, 3261−3277.
Hirata, F., & Levy, R. M. (1989) *J. Phys. Chem. 93*, 479−484.
Honig, B., & Nicholls, A. (1995) *Science 268*, 1144−1149.
Honig, B., Sharp, K., & Yang, A. (1993) *J. Phys. Chem. 97*, 1101−1109.
Irikura, K. K., Tidor, B., Brooks, B. R., & Karplus, M. (1985) *Science 229*, 571−572.
Jayaram, B., Sharp, K. A., & Honig, B. (1989) *Biopolymers 28*, 975−993.
Jayaram, B., Swaminathan, S., Beveridge, D. L., Sharp, K. A., & Honig, B. (1990) *Macromolecules 23*, 3156−3165.
Jorgensen, W. L., & Tirado-Rives, J. (1988) *J. Am. Chem. Soc. 110*, 1657−1666.
Jovin, T. M., Soumpasis, D. M., & McIntosh, L. P. (1987) *Annu. Res. Phys. Chem. 38*, 521−560.
Kennard, O., & Hunter, W. N. (1989) *Q. Rev. Biophys. 22*, 327−379.
Klapper, I., Hagstrom, R., Fine, R., Sharp, K., & Honig, B. (1986) *Proteins: Struct., Funct., Genet. 1*, 47−59.
Klement, R., Soumpasis, D. P., & Jovin, T. M. (1991) *Proc. Natl. Acad. Sci. U.S.A. 88*, 4631−4635.
Kollman, P., Weiner, P., Quigley, G., & Wang, A. (1982) *Biopolymers 21*, 1945−1969.
Krzyzaniak, A., Salanski, P., Jurczak, J., & Barciszewski, J. (1991) *FEBS Lett. 279*, 1−4.
Loprete, D. M., & Hartman, K. A. (1993) *Biochemistry 32*, 4077−4082.
Manning, G. S. (1969) *J. Chem. Phys. 51*, 924−933.
Manning, G. S. (1978) *Q. Rev. Biophys. 11*, 179−246.
Marcus, R. A. (1955) *J. Chem. Phys. 23*, 1057−1068.
Matthew, J. B., & Richards, F. M. (1984) *Biopolymers 23*, 2743−2759.
Misra, V. K., & Honig, B. (1995) *Proc. Natl. Acad. Sci. U.S.A. 92*, 4691−4695.
Misra, V. K., Hecht, J. L., Sharp, K. A., Friedman, R. A., & Honig, B. (1994a) *J. Mol. Biol. 238*, 264−280.
Misra, V. K., Sharp, K. A., Friedman, R. A., & Honig, B. (1994b) *J. Mol. Biol. 238*, 245−263.
Murthy, C. S., Bacquet, R. J., & Rossky, P. J. (1985) *J. Phys. Chem. 89*, 701−710.
Nicholls, A., Sharp, K. A., & Honig, B. (1990) *J. Comput. Chem. 12*, 435−445.
Nicholls, A., Sharp, K. A., & Honig, B. (1991) *Proteins: Struct., Funct., Genet. 11*, 281−296.
Pack, G. R., & Klein, B. J. (1984) *Biopolymers 23*, 2801−2823.
Pack, G. R., Prasad, C. V., Salafsky, J. S., & Wong, L. (1986) *Biopolymers 25*, 1697−1715.
Pohl, F. M. (1976) *Nature 260*, 365−366.
Pohl, F. M. (1983) *Cold Spring Harbor Symp. Quant. Biol. 47*, 113−118.
Pranata, J., Wierschke, S. G., & Jorgensen, W. L. (1991) *J. Am. Chem. Soc. 113*, 2810−2819.
Ramstein, J., & Leng, M. (1980) *Nature 288*, 413−414.
Record, M. T., Anderson, C. F., & Lohman, T. M. (1978) *Q. Rev. Biophys. 11*, 103−178.
Rich, A., Nordheim, A., & Wang, A. H.-J. (1984) *Annu. Rev. Biochem. 53*, 791−846.
Saenger, W., Hunter, W. N., & Kennard, O. (1986) *Nature 324*, 385−388.
Sharp, K. A., & Honig, B. (1990a) *J. Phys. Chem. 94*, 7684−7692.
Sharp, K. A., & Honig, B. (1990b) *Annu. Rev. Biophys. Biophys. Chem. 19*, 301−332.
Sharp, K. A., Honig, B., & Harvey, S. C. (1990) *Biochemistry 29*, 340−346.
Soumpasis, D. M. (1984) *Proc. Natl. Acad. Sci. U.S.A. 81*, 5116−5120.
Soumpasis, D. M. (1988) *J. Biomol. Struct. Dyn. 6*, 563−574.
Stirdivant, S. M., Klysik, J., & Wells, R. D. (1982) *J. Biol. Chem. 257*, 10159−10165.
Thomas, T. J., & Bloomfield, V. A. (1983) *Nucleic Acids Res. 11*, 1919−1930.
Umehara, T., Kuwabara, S., Mashimo, S., & Yagihara, S. (1990) *Biopolymers 30*, 649−656.
Vlachy, V., & Haymet, A. D. T. (1986) *J. Chem. Phys. 84*, 5874−5880.
Wang, A. H.-J., Quigley, G. J., Kolpak, F. J., van der Marel, G., van Boom, J. H., & Rich, A. (1981) *Science 211*, 171−176.
Weiner, S. J., Kollman, P. A., Nguyen, D. T., & Case, D. A. (1986) *J. Comput. Chem. 7*, 230−252.
Westhof, E. (1988) *Annu. Rev. Biophys. Biophys. Chem. 17*, 125−144.
Zacharias, M., Luty, B. A., Davis, M. E., & McCammon, J. A. (1992) *Biophys. J. 3*, 1280−1285.
Zacharias, W., Larsson, J. E., Klysik, J., Stirdivant, S. M., & Wells, R. D. (1982) *J. Biol. Chem. 257*, 2775−2782.
Zacharias, W., O'Connor, T. R., & Larsen, J. E. (1988) *Biochemistry 27*, 2970−2978.

BI951463Y